Ocean Sci. J. (2017) 52(2):177–192
http://dx.doi.org/10.1007/s12601-017-0020-9

Article

Available online at http://link.springer.com
SpringerLink

Ocean Science Journal
pISSN 1738-5261
eISSN 2005-7172

Tracing the Origin of Pb using Stable Pb Isotopes in Surface Sediments along the Korean Yellow Sea Coast

Jong-Kyu Park[1], Man-Sik Choi[1]*, Yunho Song[2], and Dhong-Il Lim[3]

[1]*Department of Ocean Environmental Sciences, College of Natural Sciences, Chungnam National University, Daejeon 34134, Korea*
[2]*Advanced Geo-materials R&D Department, Pohang Branch, Institute of Geoscience and Mineral Resources, Pohang 37559, Korea*
[3]*Library of Marine Samples, South Sea Research Institute, KIOST, Geoje 53201, Korea*

Received 11 Novermber 2016; Revised 8 February 2017; Accepted 9 February 2017

Abstract – To investigate the factors controlling lead (Pb) concentration and identify the sources of Pb in Yellow Sea sediments along the Korean coast, the concentration of Pb and Pb isotopes in 87 surface and 6 core sediment samples were analyzed. The 1 M HCl leached Pb concentrations had a similar geographic distribution to those of fine-grained sediments, while the distribution of residual Pb concentrations resembled that of coarse-grained sediments. Leached Pb was presumed to be associated with manganese (Mn) oxide and iron (Fe) oxy/hydroxide, while residual Pb was associated with potassium (K)-feldspar, based on good linear relationships between the leached Pb and the Fe/Mn concentrations, and the residual Pb and K concentrations. Based on a ratio–ratio plot with three isotopes ($^{207}Pb/^{206}Pb$ and $^{208}Pb/^{206}Pb$) and the geographic location of each sediment, sediments were categorized into two groups of samples as group1 and group2. Group 1 sediments, which were distributed in Gyeonggi Bay and offshore (north of 36.5°N), were determined to be a mixture of anthropogenic and natural Pb originating from the Han River, based on a $^{208}Pb/^{206}Pb$ against a $Cs/Pb_{leached}$ mixing plot of core and surface sediments. Group 2 sediments, which were distributed in the south of 36.5°N, also showed a two endmembers mixing relationship between materials from the Geum River and offshore materials, which had very different Pb concentrations and isotope ratios. Based on the isotopes and their concentrations in core and surface sediments, this mixing relationship was interpreted as materials from two geographically different origins being mixed, rather than anthropogenic or natural mixing of materials with the same origin. Therefore, the relative percentage of materials supplied from the Geum River was calculated using a two endmembers mixing model and estimated to be as much as about 50% at 35°N. The spatial distribution of materials derived from the Geum River represented that of fine-grained sediments originating from the Geum River. It was concluded that Pb isotopes in sediments could be used as a tracer in studies of the origin of fine-grained sediments along the Korean Yellow Sea coast.

*Corresponding author. E-mail: mschoi@cnu.ac.kr

Key words – Pb, sediments, Pb isotopes, the Yellow Sea

1. Introduction

Coastal environments are important reservoirs for many persistent contaminants, including metals, which might accumulate in organisms and bottom sediments (Liu et al. 2011; Gao et al. 2014; Alyazichi et al. 2015). In marine environments, metals are largely associated with particulate matter (Gibbs 1973; Gerritse et al. 1998; Nagano et al. 2003; Tarras-Wahlberg and Lane 2003). Sources of particulate matter in coastal areas include local river discharges, suspended particulate matter in the oceanic water column, and particles derived from atmospheric deposition (Sindern et al. 2016). Lead (Pb) is one of the most widely used metals in industrial activities and accompanies economic development and population growth (Cheng and Hu 2010). As a result, it has become the most widely distributed toxic element in the global environment and has thus received much public attention. The identification of the sources, controlling factors, and pathways of Pb are important for maintaining the coastal environment.

Pb has four stable isotopes, ^{204}Pb, ^{206}Pb, ^{207}Pb, and ^{208}Pb. While ^{204}Pb is naturally present in the crust, the other three isotopes are the stable daughter products of the radioactive decay of ^{238}U, ^{235}U, and ^{232}Th, respectively (Patterson 1955). Because Pb isotope ratios might differ between sources and the isotope ratio is relatively unaffected by physicochemical fractionation processes, Pb isotopes have been used to identify sources of Pb and to determine the transport pathways of Pb using marine materials including seawater, aerosols, organisms,

and sediments (Hamilton and Clifton 1979; Flegal et al. 1987; Hamelin et al. 1990; Labonne et al. 1998; Munksgaard et al. 1998; Hinrichs et al. 2002; Choi et al. 2007).

The Yellow Sea is an epicontinental shelf surrounded by mainland China and the Korean Peninsula, which receives billions of tons of particulate materials on an annual basis from surrounding rivers (the Huanghe and Changjiang rivers, as well as various Korean rivers; Lee and Chough 1989). In addition to rivers, atmospheric inputs also supply annually millions of tons of particulate materials to the Yellow Sea (Gao et al. 1992; Zhang et al. 1992). Choi et al. (2007) identified Pb sources in river mouth sediments of Chinese and Korean rivers and shelf sediments, based on Pb isotopes in the Yellow Sea. Several subsequent studies of marine sediments, mainly those undertaken along the Chinese coast of the Yellow Sea, have reported increasing levels of anthropogenic Pb from energy consumption, including vehicle emissions and coal combustion in the Yangtze River estuary (Zhang et al. 2008; Hao et al. 2008), the Yellow River estuary near the Bohai Sea (Hu et al. 2015a), Liaodong Bay (Hu et al. 2015b), western Xiamen Bay (Hu et al. 2013), and Quanzhou Bay (Yu et al. 2016).

However, there are no reports of Pb isotope levels in Yellow Sea sediments from the Korean coast. It has been speculated that Pb isotopes in sediments could be used to discriminate between materials from the Han and Geum Rivers (Choi et al. 2007). Since Pb isotopes in the sediments from each river resembled those in local ores in the drainage basin of each river, the areal extent of materials from the two rivers would be determined by Pb isotopes. In addition, Pb concentrations in the 1 M HCl leached fraction of sediments varies depending on grain size and might be controlled by the iron (Fe) oxy/hydroxide content (Kim et al. 2000; Choi et al. 2007). Thus, it might be expected that Pb isotopes in the 1 M HCl leached fraction of sediments might indicate the sources of fine-grained sediments, if Pb and fine-grained particles behave similarly in this dynamic coastal area.

Therefore, this study attempted to identify the sources of Pb in Yellow Sea sediments from the Korean coast using Pb isotopes and the factors controlling Pb concentrations in sediments.

2. Study Area

The Yellow Sea is an epicontinental shelf, with a mean water depth of 55 m and a maximum depth of 100 m. There are many rivers draining the China mainland and Korean Peninsular such as Chinese rivers (e.g. the Huanghe, Changjiang, etc) and Korean rivers (e.g. the Han, the Geum, etc). Although at present the Changjiang and the Huanghe rivers do not directly empty sediments into the Yellow Sea, they were a major source of sediment in the Yellow Sea during the Holocene (Milliman et al. 1985a, 1987; Ren and Shi 1986; Yang 1989; Alexander et al. 1991a, 1991b; Martin et al. 1993). However, in the eastern part of the Yellow Sea, because Korean rivers discharge a smaller amount of sediment than Chinese rivers (Schubel et al. 1984; Ren and Shi 1986), the long-range transport of materials from Chinese rivers is likely to be important for the Korean coast (Cho et al. 1999).

The eastern part of the Yellow Sea is characterized by numerous islands bounded by tidal flats along the Korean coast (Lee et al. 1988; Chough et al. 2000). Tides are typically semi-diurnal (M2), with a tidal range of 4 to 8 m (Chough et al. 2000), and tidal currents flow northward during flood tides and mostly south to southwestward during ebb tides (Park and Lee 1994; Lee and Chu 2001). These currents form a clockwise gyre consisting of the Yellow Sea Warm Current and the southward inflow of the Korea Coastal Current (KCC). The KCC flows southward along 40–50 m isobaths in the eastern Yellow Sea, greatly influencing sediment transport along the Korean coast (Chough and Kim 1981; Wells 1988; Lee and Chough 1989).

The distribution and origin of Yellow Sea sediments has been reported in several studies (Yang et al. 2003, and references therein). Coarse-grained transgressive sandy deposits formed during the last postglacial rise in sea level and are distributed throughout the northeastern Yellow Sea (Lee et al. 1988; Chough et al. 2000), resulting in ubiquitous tidal sand ridges in this region (Klein et al. 1982; Chough et al. 2000). Fine-grained muddy deposits, referred to as southeastern Yellow Sea mud (SEYSM), are distributed throughout the southeastern Yellow Sea (Lee and Chough 1989; Gao et al. 1992; Park and Khim 1992).

The Yellow Sea has suffered from the effects of rapid industrialization and urbanization in its coastal regions (Kim et al. 2000; Choi et al. 2007; Yuan et al. 2012; Zhang et al. 2012). Thus, environmental issues have arisen in relation to the input of various pollutants to the marine environment (Kim et al. 2000). On the Korean coast of the Yellow Sea, huge dykes have been constructed at Saemangeum and Shiwha, which have caused many environmental changes and problems, such as red tides, the degradation of natural

habitats, a decline in water quality, restricted water circulation, tidal excursions, and sediment transport (Choi et al. 1997; Yoo et al. 2002; Yih et al. 2005; Lee and Ryu 2008; Baek et al. 2011; Lee and Lee 2012; Lee et al. 2014; Jeong and Yang 2015). Coal-fired power plants have also been constructed in Boryeong, Dangjin, Taean, Seocheon, and Pyeongtak.

Therefore, the marine environment along the Korean coast of the Yellow Sea has been affected by numerous anthropogenic activities, and it has become essential to establish environmental management plans that include the identification of pollutant sources.

3. Materials and Methods

Eighty-seven surface sediment samples and six core sediments were collected using a Van Veen grab sampler and a gravity corer, respectively, during 2007–2009. Surface sediment samples were frozen in vinyl bags until analysis. Core sediments were sliced to a thickness of 1–2 cm and frozen. Sediment samples were freeze-dried, powdered in an agate mortar, and stored in plastic vials until analysis.

Choi et al. (2007)'s method was used to analyze the concentrations of Fe, aluminum (Al), cesium (Cs), manganese (Mn), and Pb in bulk sediments, as well as Pb isotopes and Pb concentrations in the 1 M HCl leached fraction. In brief, a 0.2 g powdered sediment was placed into a 60 mL Teflon digestion vessel (Savillex, Eden Prairie, MN, USA) and then digested overnight with 4 mL mixed acids (HNO_3:$HClO_4$ = 3:1) on a hot plate at 170°C. After the digested solution was fully dried, residual solids were digested with 4 mL mixed acids (HF:$HClO_4$ = 3:1) under the same conditions. The digested solution was fully dried, and this step was repeated twice. After evaporation, residual solids were reacted with 1 mL $HClO_4$ and 5 mL saturated boric acid to remove residual fluorides and then extracted using 20 mL 1% HNO_3 solution. To analyze leached metals, the 0.2 g powdered sample was placed into 60 mL centrifuge tubes and reacted with 20 mL 1 M HCl in a horizontal shaker at room temperature

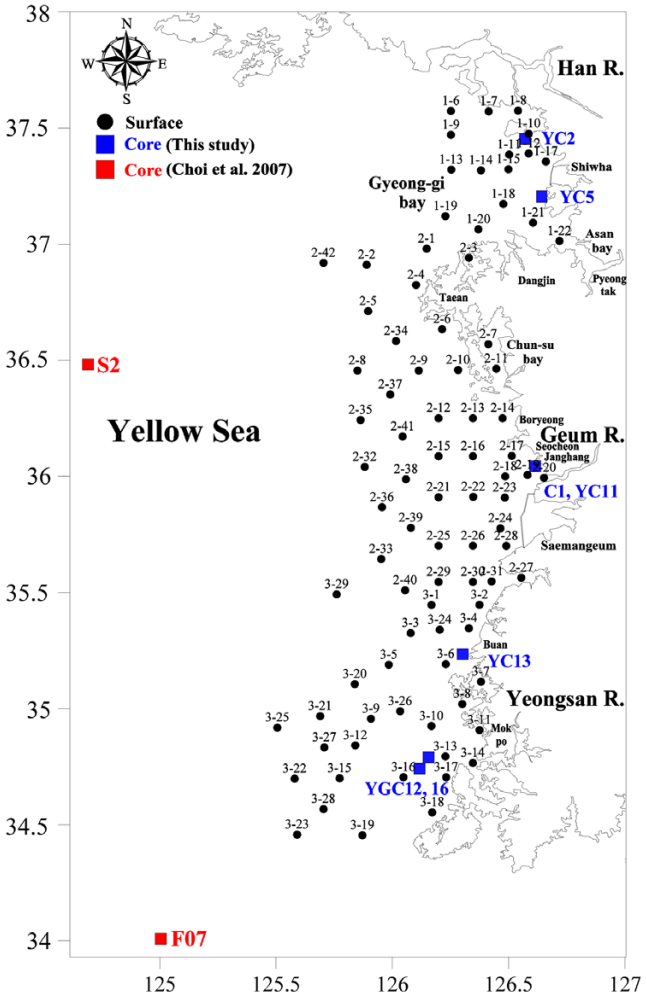

Fig. 1. Map of the sampling sites. Surface (dots) and core (squares) sampling site names are marked

for 24 h. After centrifugation, the supernatants were collected and then diluted using 10 mL 1% HNO_3. Residual Pb was used to obtain leached Pb.

Metals in both the bulk digested sample and the 1 M HCl leached fraction were measured by inductively coupled plasma atomic emission spectrometry (ICP-AES; Optima 4300 DU; Perkin-Elmer Ltd., Waltham, MA, USA) and inductively coupled plasma mass spectrometry (ICP-MS;

Table 1. Pb concentration and Pb isotope ratios for reference materials

	Pb (mg/kg)	$^{207}Pb/^{206}Pb$	$^{208}Pb/^{206}Pb$
NBS 981 (n = 9)		0.91456 ± 0.0001	2.1662 ± 0.00002
Certified value		0.91464 ± 0.0003	2.1681 ± 0.0008
MESS-3 (n = 6)	18.25	0.8116	2.0227
stdev.	0.37	0.0001	0.0004
Certified value	21.1		
% recovery	86		

X-5; Thermo Elemental Ltd., Winsford, UK) at the Korea Basic Science Institute (KBSI). Instrumental drift and matrix effects during measurement were corrected using a ^{205}Tl internal standard. The $^{207}Pb/^{206}Pb$ and $^{208}Pb/^{206}Pb$ ratios in the 1 M HCl leached fraction were measured by multi-collector inductively coupled plasma mass spectrometry (MC-ICP-MS; Neptune, ThermoFinnigan Ltd., UK.) in the KBSI after spiking with Tl (NIST SRM 997) to correct for instrumental mass bias. The quality-control results are summarized in Table 1.

4. Results

Spatial distribution of Al, Fe, Mn, $CaCO_3$, C_{org}, and Cs concentrations in surface sediments

Grain size is one of most important factors controlling trace metal concentrations in Korean coastal sediments (Loring 1990; Kim et al. 1998; Cho et al. 1999; Song et al. 2011, 2014). The levels of some refractory metals, such as Al, Fe, magnesium, lithium, and Cs have been used instead of grain size parameters to explain grain size distribution, because their concentrations are usually strongly correlated with the latter (Lim et al. 2007; Song et al. 2014). Cs has been used as a geochemical normalizer of grain size along the southern coast of Korea (Song et al. 2014). Thus, we used Cs concentration to investigate the spatial distribution of grain size. In addition, the spatial distributions of other geochemical substrates, such as clay minerals (Al concentration), Fe-Mn oxy/hydroxides (Fe and Mn concentrations), organic matter (C_{org}), and $CaCO_3$ were analyzed (Fig. 2) to determine the Pb distribution.

Cs concentrations ranged from 0.7 to 10.3 mg/kg (mean: 3.7 ± 2.3 mg/kg). Generally, the Cs concentration was lower north of 35.5°N than in the south, and it was also lower in offshore than that in coastal areas north of 35.5°N. It was lower in coastal areas than that in offshore in the south (Fig. 2a). The spatial distribution of Cs concentration was generally similar to that of grain size (Cs = 0.99 × mean grain size – 0.24, $r^2 = 0.70$), with sand deposits in the offshore area north of 35.5°N and fine-grained muddy deposits in the offshore area in the south, which is referred to as the SEYSM or Heuksan Mud Belt (HMB) (Lee and Chough 1989).

Al and Fe concentrations varied from 2.0% to 9.9% (mean: 5.8% ± 1.7%), and from 0.3% to 4.4% (mean: 2.1% ± 1.1%), respectively, showing a similar spatial distribution to the Cs concentration (Fig. 2b and 2c).

$CaCO_3$ concentrations varied from 0.05% to 22.5% (mean: 1.70 ± 3.6%). Relatively high concentrations (> 1%) were found along the coastlines north of 35.5°N and in sediments collected near islands in the south (Fig. 2d).

The C_{org} concentration in sediments ranged from 0.01% to 1.3% (mean: 0.3 ± 0.2%). In the north of 35.5°N, relatively lower concentrations were found at offshore sites than in coastal area. But the opposite spatial distribution was apparent in the south. Generally, the spatial distribution of C_{org} concentration was similar to that of Cs (Fig. 2e) The Mn concentration ranged from 94 to 9967 mg/kg (mean 664 ± 1231.8 mg/kg), but most samples had a concentration lower than 2000 mg/kg, excluding two anomalously enriched samples (3-9, 3-12). For samples with a $CaCO_3$ content < 4%, Mn concentrations were correlated linearly with the $CaCO_3$ content (r = 0.70) (Fig. 2f).

Spatial distribution of leached, residual, and total Pb concentrations in surface sediments

Since a relatively high concentration of Pb can exist within the crystal lattices of alumino-silicate minerals (e.g., potassium [K]-feldspar) (Hinrichs et al. 2002), and has been reported in the sandy Yellow Sea sediments (Kim et al. 2000; Choi et al. 2007), a leaching procedure using 1 M HCl solution at room temperature was adopted. This leaching procedure has been widely used because it can extract the environmentally labile fraction in bulk sediments (Shirahata et al. 1980; Ng and Patterson 1982; Hamelin et al. 1990; Kober et al. 1999; Sutherland 2002), and had little effect on the alumino-silicate lattice.

The Pb concentration was measured in both the leached and residual fractions as in Choi et al. (2007). The spatial distribution of leached Pb ($Pb_{leached}$), residual Pb (Pb_{res}), and the total Pb (Pb_t) concentration are shown in Fig. 3.

The $Pb_{leached}$ concentrations ranged from 3.8 to 28.8 mg/kg (mean: 11.3 ± 5.3 mg/kg), with higher concentrations in coastal areas than offshore north of 35.5°N, while the opposite pattern was apparent in the south, which was similar to the spatial distribution of Cs. The lowest Pb concentrations were found at offshore sites north of 35.5°N, where widespread sand deposits were present (Dong et al. 1989; Gao et al. 1996). A relatively high $Pb_{leached}$ concentration was found in coastal areas in Gyeonggi Bay and from Chunsu Bay to the Geum River mouth. In addition, the highest $Pb_{leached}$ concentrations were found at offshore sites in the south.

The Pb_{res} concentration varied from 2.6 to 18.1 mg/kg (mean: 11.1 ± 3.6 mg/kg), with a lower concentration south

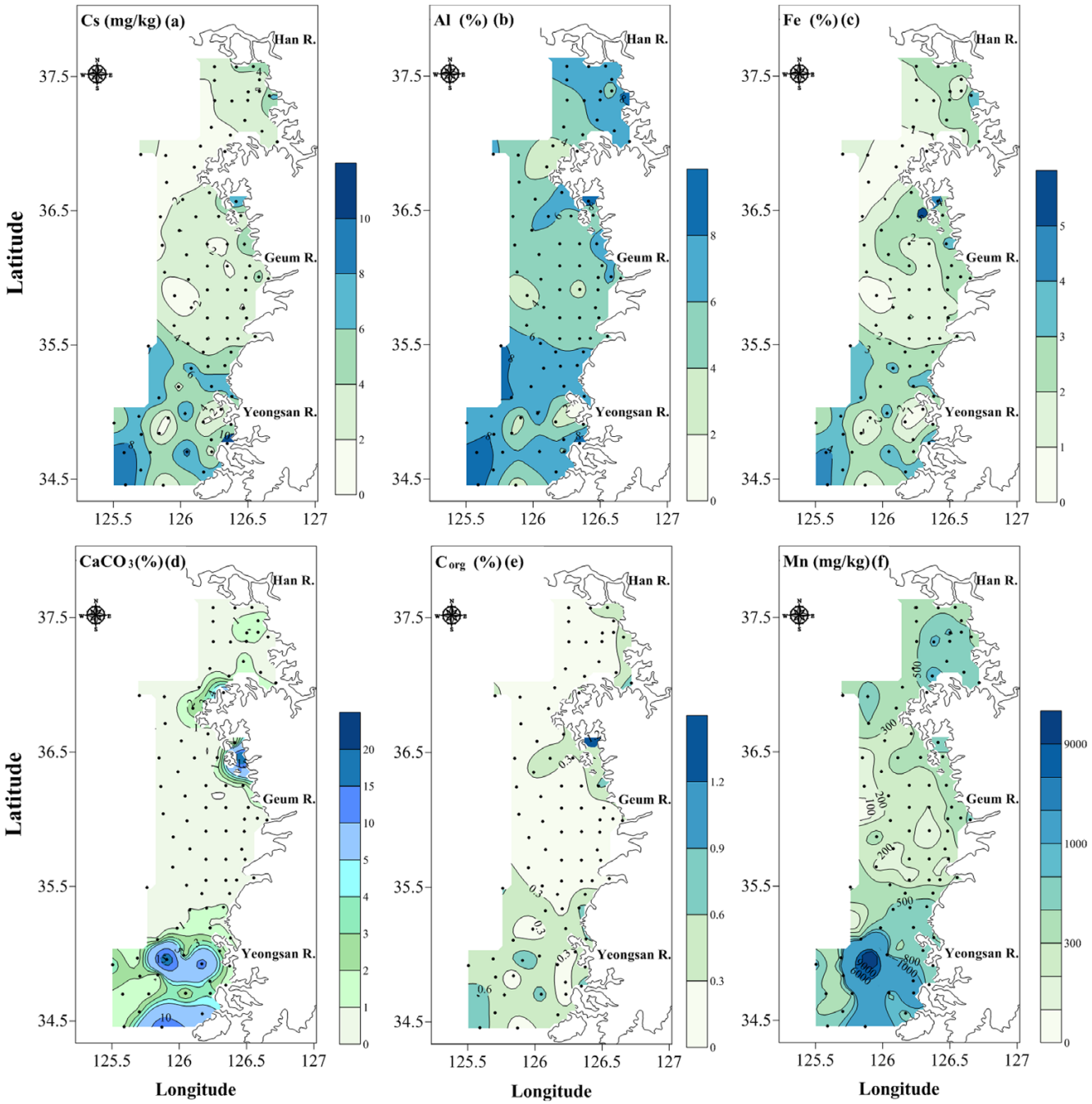

Fig. 2. Spartial distribution of Cs (mg/kg), Al (%), Fe (%), $CaCO_3$ (%), C_{org} (%), and Mn (mg/kg) concentrations in surface sediments

of 35.5°N than north of it and the opposite spatial distribution to that of the $Pb_{leached}$ and Cs concentrations.

Because the spatial distributions of the leached and Pb_{res} concentrations mirrored each other, the Pb_t concentration varied within a small range (14.6–33 mg/kg, mean: 22.5 ± 3.7 mg/kg), and was relatively high at sites with a high $Pb_{leached}$ concentration (coastal areas in the north and offshore areas in the south) and at sites with high Pb_{res} concentrations (offshore areas in the north). Thus, the grain size dependence of the Pb_t concentration, such as that expressed for Mn, strontium, and barium, could not be identified in sediments in the study area (Lee et al. 1992; Kim et al. 1998).

Spatial distribution of stable Pb isotopes in the 1 M HCl leached fraction

The spatial distributions of the $^{207}Pb/^{206}Pb$ and $^{208}Pb/^{206}Pb$

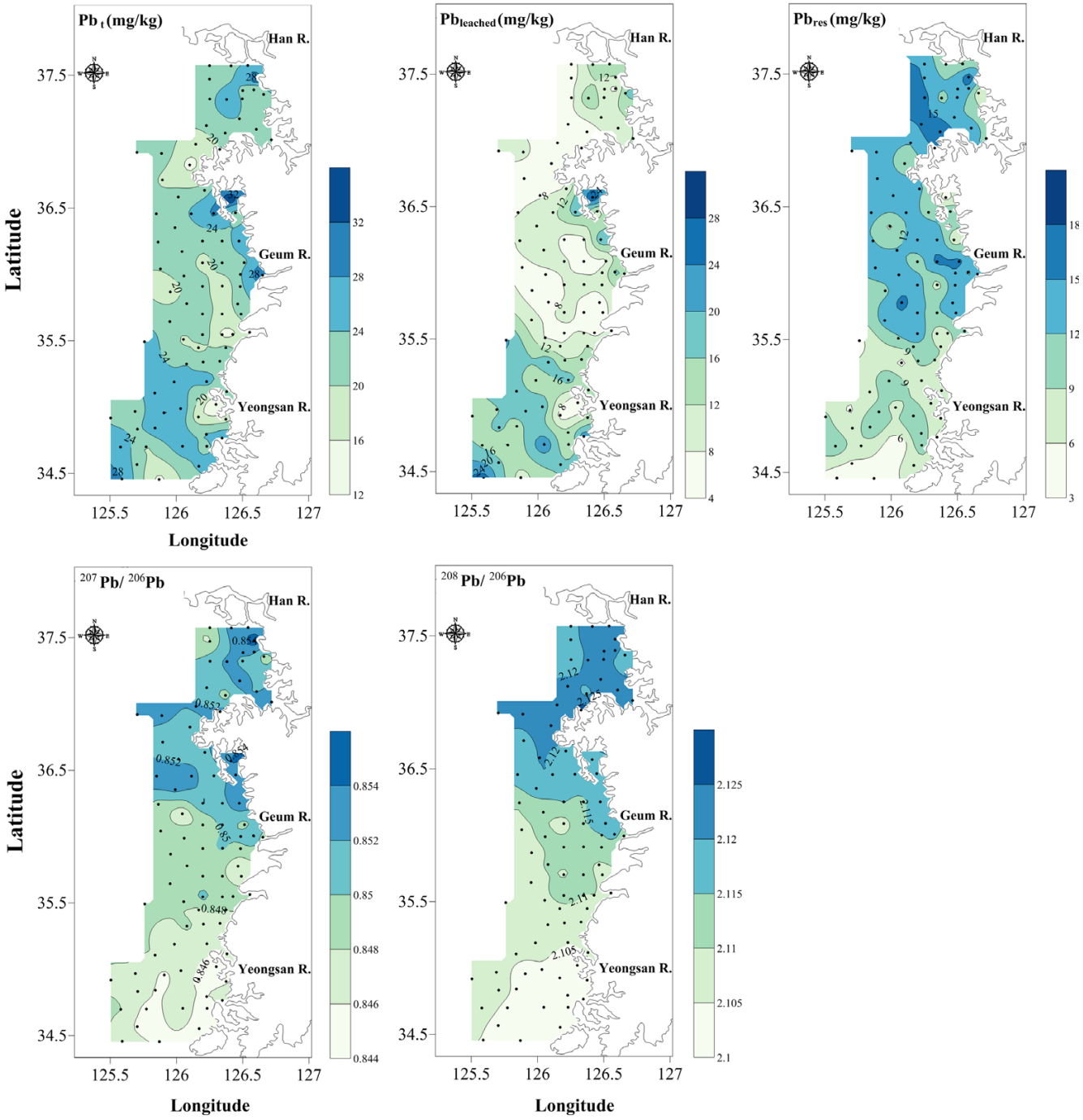

Fig. 3. Spatial distribution of $Pb_{leached}$, Pb_{res}, and Pb_t concentrations and Pb isotope ratios ($^{207}Pb/^{206}Pb$ and $^{208}Pb/^{206}Pb$) in surface sediments

ratios in the 1 M HCl leached fraction are shown in Fig. 3; they ranged from 0.8439 to 0.8554 (mean: 0.8494 ± 0.0027) and 2.1002 to 2.1265 (mean: 2.1125 ± 0.0069), respectively. The highest values were found at the northernmost sites, and they decreased toward the south (Fig. 3). The characteristic features of the spatial distribution can be summarized as follows. There was greater spatial variation in the $Pb_{leached}$, Pb_{res}, Cs, C_{org}, Al, and Fe concentrations in the north–south direction than in the east–west direction, which indicates that there was little grain size dependence in the isotope ratios. The gradient of the isotope ratio was not consistent with that of the $Pb_{leached}$ concentration, which indicates that there were mixing relationships among sources with different isotope ratios and $Pb_{leached}$ concentrations. Finally, the Pb isotope ratios

in sediments at the Geum River mouth had intermediate values compared to those in the northernmost and southernmost areas.

Depth profiles of Pb isotopes, Cs concentration, and leached and total Pb concentration

The vertical profiles of $Pb_{leached}$, Pb_t, and Cs concentrations and Pb isotope ratios in six core sediments are shown in Fig. 4. In the YC2 core, which was collected in Gyeonggi Bay, metal concentrations varied from 8.5 to 12.9 mg/kg (mean: 10.6 ± 1.4 mg/kg) for $Pb_{leached}$, 20.6 to 22.1 mg/kg (mean: 21.4 ± 0.5 mg/kg) for Pb_t, and 4.3 to 5.9 (mean: 5.1 ± 0.5 mg/kg) for Cs. Although no upward increase in $Pb_{leached}$ and Pb_t concentrations was observed, $^{207}Pb/^{206}Pb$ and $^{208}Pb/^{206}Pb$ ratios increased from 0.8463 to 0.8528 and 2.1161 to 2.1227, respectively, from 20 cm to the surface.

In the YC5 core, which was collected in Asan Bay, metal concentrations varied from 6 to 9.8 mg/kg (mean: 8.2 ± 1.4 mg/kg) for $Pb_{leached}$, 16.2 to 18 mg/kg (mean: 16.9 ± 0.5 mg/kg) for Pb_t, and 2.7 to 4 mg/kg (mean: 3.4 ± 0.5 mg/kg) for Cs. Pb_t and $Pb_{leached}$ concentrations showed little variability, but the $^{207}Pb/^{206}Pb$ and $^{208}Pb/^{206}Pb$ ratios were generally high at the surface and low at depth.

In the YC11 core, which was collected at the Geum River mouth, metal concentrations varied from 10.8 to 21.6 mg/kg (mean: 16.1 ± 3.8 mg/kg) for $Pb_{leached}$, 27.2 to 41.3 mg/kg (mean: 33.8 ± 5 mg/kg) for Pb_t, and 4.2 to 5.2 mg/kg (mean: 4.6 ± 0.3 mg/kg) for Cs. The Pb_t and $Pb_{leached}$ concentrations decreased gradually toward the surface, while the isotope ratios decreased slightly toward the surface.

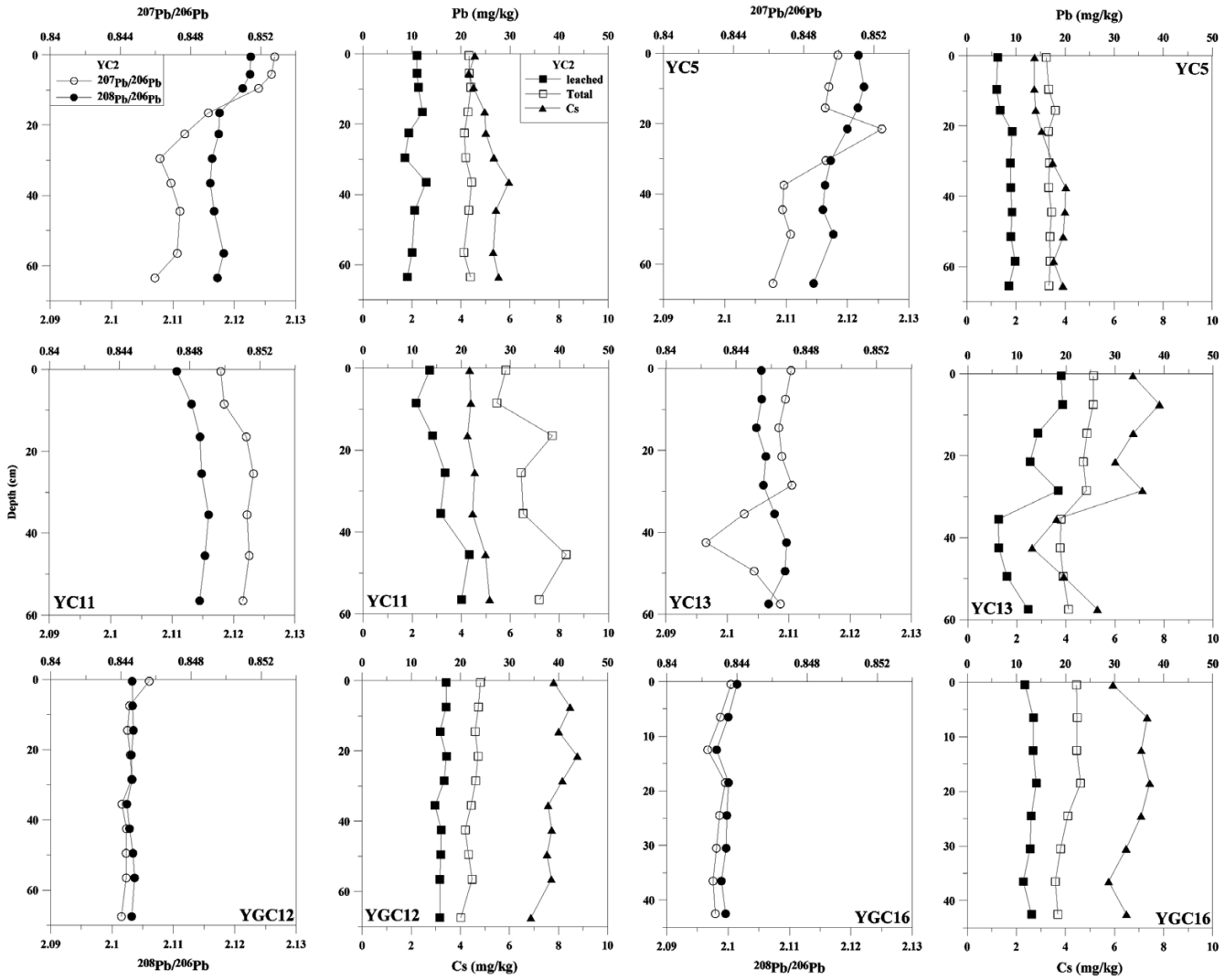

Fig. 4. Vertical profiles of Cs, $Pb_{leached}$, and Pb_t concentrations and Pb isotope ratios ($^{207}Pb/^{206}Pb$ and $^{208}Pb/^{206}Pb$) in core sediments

In the YC13 core, which was collected in the coastal area in Buan, metal concentrations varied from 6.2 to 19.3 mg/kg (mean: 12.9 ± 5.3 mg/ kg) for $Pb_{leached}$, 18.8 to 25.6 mg/kg (mean: 22.3 ± 2.8 mg/kg) for Pb_t, and 2.6 to 7.8 mg/kg (mean: 5.5 ± 1.8 mg/kg) for Cs. The $Pb_{leached}$ and Pb_t concentrations increased abruptly at a depth of 30 cm, following the increase in the Cs concentration, indicating a change in grain size. In addition, isotope ratios changed at a depth of 30 cm.

In the YGC12 core, which was collected in the coastal area off Mokpo, metal concentrations varied from 14.8 to 17.1 mg/kg (mean: 16.2 ± 0.7 mg/kg) for $Pb_{leached}$, 20.1 to 24.1 mg/kg (mean: 22.5 ± 1.3 mg/kg) for Pb_t, and 6.9 to 8.8 mg/kg (mean: 7.9 ± 0.5 mg/kg) for Cs. The $^{207}Pb/^{206}Pb$ and $^{208}Pb/^{206}Pb$ ratios varied slightly in the range of 0.8440 to 0.8456 (mean: 0.8445 ± 0.0004) and 2.1024 to 2.1037 (mean: 2.1032 ± 0.0004), respectively.

In the YGC16 core, which was collected from a site near to the YGC12 core, metal concentrations varied from 11.4 to 14 mg/kg (mean: 12.9 ± 0.9 mg/kg) for $Pb_{leached}$, 17.9 to 23.1 (mean: 20.7 ± 2 mg/kg) for Pb_t, and 5.8 to 7.4 (mean: 6.7 ± 0.6 mg/kg) for Cs. The $^{207}Pb/^{206}Pb$ and $^{208}Pb/^{206}Pb$ ratios varied slightly in the range of 0.8423 to 0.8437 (mean: 0.8429 ± 0.0004) and 2.0981 to 2.1014 (mean: 2.0997 ± 0.0009), respectively.

5. Discussion

Factors controlling Pb concentrations in surface sediments

From the spatial variation in leached and Pb_{res} concentrations in the study area, it was apparent that each species responded in an opposite manner to its grain size. Thus, the concentration of three fractions of Pb were directly comparable with the Cs concentration, indicating the distribution of grain size (Fig. 5a). The $Pb_{leached}$ concentration was positively correlated with the Cs concentration, while the Pb_{res} concentration and Cs concentration were negatively correlated; thus, the Pb_t concentration had little dependence on the Cs concentration.

Although environmentally labile Pb would be hosted by a Fe/Mn oxy/hydroxide in an oxic environment (Kim et al. 2000), or in sulfides in a polluted or organic-rich environment, and anoxic sediments (Calvert 1976), the presence of Fe/Mn oxy/hydroxide is more likely important to the distribution of labile Pb than that of sulfides because of the high tidal activity in the Yellow Sea coastal region. In addition, the Pb_t concentrations found in this study were lower than those in polluted regions such as Shiwha Lake and Incheon Harbor (Ahn et al. 1995; Jung et al. 1996; Choi et al. 1999).

Fe and Mn, because of their abundance in rocks and their low solubility over the range of seawater pH values, tend to form the most important oxide, oxy/hydroxide, and hydroxide minerals in sediments (Koon et al. 1980). In addition, Pb is quite reactive and adsorbs onto particulate materials, particularly to Fe-Mn oxy/hydroxide (Carpenter et al. 1975; Bargar et al. 1997; Ewais et al. 2000; Dong et al. 2003; Négrel and Petelet-Giraud 2012). Because this study did not acquire the leached Fe concentration, the $Pb_{leached}$ concentration was compared to the excess Fe concentration obtained from the following equation (Fig. 5b): $Fe_{ex}(\%) = Fe_t(\%) - (Fe/Al)_{\text{lowest value in this study}} \times Al(\%)$.

Because the $Pb_{leached}$ concentration was strongly correlated with excess Fe (except for the four samples marked by dotted circles in Fig. 5b), it might be suggested that $Pb_{leached}$ was preferentially adsorbed onto the Fe oxy/hydroxide (Kim et al. 2000). Based on the relationships between Mn and $Pb_{leached}$ concentrations shown in Fig. 5c, the four excluded samples in Fig. 5b have an anomalously high Mn concentration, ranging from 1,300 to 9,967 mg/kg. Because Mn also has a strong tendency to scavenge metals, it might be concluded that the $Pb_{leached}$ concentration was controlled by not only Fe oxy/hydroxide but also Mn oxide.

Next, the Pb_{res} concentration was compared to the K concentration after being normalized against the Cs concentration (Fig. 5d), because K can be hosted in a very different grain-size fraction (Calvert 1976). The linear relationship between the Pb_{res} and K concentrations suggests that the Pb_{res} was also hosted in a lattice of K-containing minerals, such as K-feldspar (Kim et al. 2000).

Identification of endmembers and mixing relationships

To identify the sources of Pb in sediments, mixing relationships and possible endmembers were estimated from the isotope ratios in both surface and core sediments by comparing the ratios with possible source-related materials (Fig. 6a). The possible source-related materials were surface sediments at the mouths of the Han and Geum rivers, offshore core sediments (S2, F07), surface sediments, and suspended materials at the mouths of two Chinese rivers, Huanghe and Changjiang (Choi et al. 2007). Atmospheric particulate matter (APM) from major cities in China and Korea might also be possible sources, and therefore the average Pb isotope ratios of aerosols collected in Beijing, Tianjian, Shanghai, and Seoul (Choi et al. 2007) were compared.

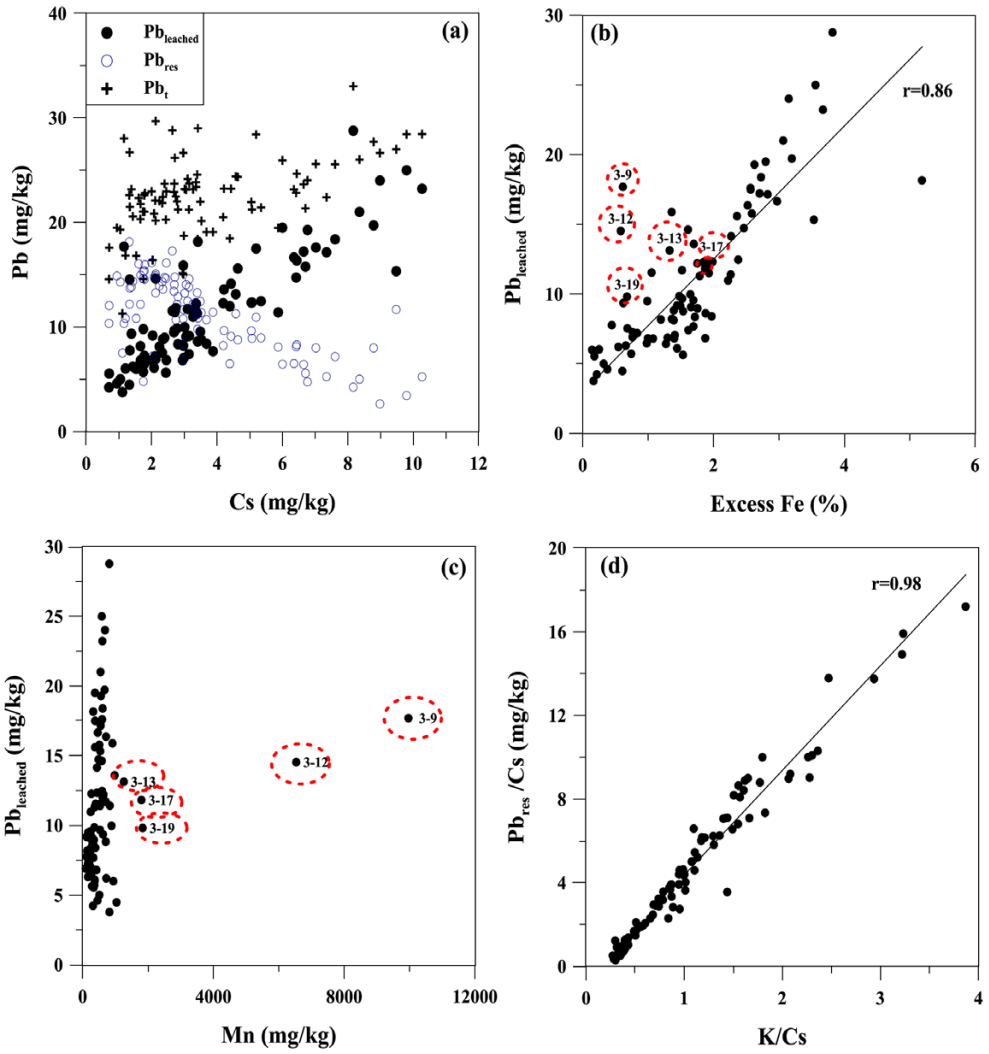

Fig. 5. The interrelationships between Pb species and Cs concentration (a), between $Pb_{leached}$ and excess Fe (b) and Mn (c), and between Pb_{res} and the K/Cs ratio (d)

Pb isotope ratios in river mouth sediments from Korean (Han and Geum) and Chinese (Huanghe and Changjiang) rivers were distinctly different, enabling the discrimination of sediments, because most of the $Pb_{leached}$ in river mouth sediments originated from local ores in each drainage basin (Choi et al. 2007; Fig. 6a). In addition, Pb isotopes in river mouth sediments could be distinguished from APM from the major cities of China and Korea. When Pb isotopes in surface and core sediments were compared in the possible source-related materials, it was found that all of the sediment samples contained more thorogenic Pb isotopes (higher slope in Fig. 6a) than samples from Chinese rivers. The highest isotope ratios were consistently found in the Han and Geum river mouth sediments, and the lowest values were found in core F07 from the southern offshore core sediments (Fig. 6a). In addition, Pb isotope ratios in the deep (40–65 cm) samples of cores YC2 and YC5 were consistent with endmember confining sediments collected at Gyeonggi Bay and the other endmembers of the Han River mouth sediments (within the rectangular area in Fig. 6a). Thus, the samples, including surface and core sediments, could be categorized into two groups, which could be distinguished geographically, one north of 36.5°N and the other south of 36.5°N. Therefore, this result indicated that two mixing series existed.

The first group consisted of samples with the two endmembers of the Han River mouth sediments (0.8545 ± 0.0014 and 2.1239 ± 0.0031 for $^{207}Pb/^{206}Pb$ and $^{208}Pb/^{206}Pb$, respectively) and the deep sediments of cores YC2 and YC5 (0.8476 ± 0.0023 and 2.1178 ± 0.0037 for $^{207}Pb/^{206}Pb$ and $^{208}Pb/^{206}Pb$, respectively), which were distributed within

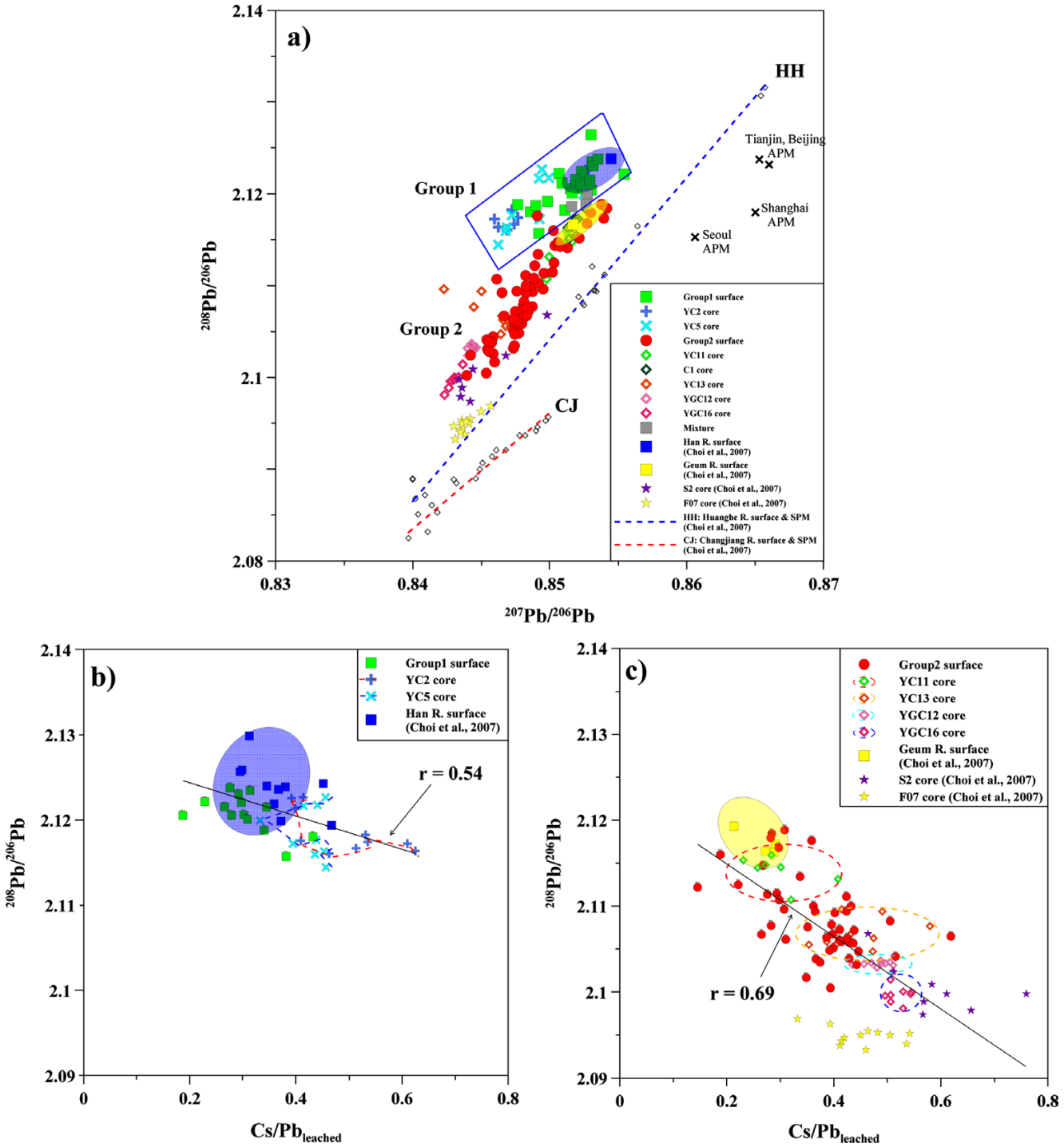

Fig. 6. The ratio–ratio plot using three isotopes ($^{207}Pb/^{206}Pb$ and $^{208}Pb/^{206}Pb$) (a), $^{208Pb}/^{206}Pb$ versus $Cs/Pb_{leached}$ for group 1 sediments (b), and for group 2 sediments (c). The shadowed areas indicate the ranges of Pb isotope ratios and concentrations for materials originated from the Han River (blue) and the Geum River (yellow)

Gyeonggi Bay. The second group included mixed sediments with the two endmembers of the Geum River mouth sediments (0.8517 ± 0.0013 and 2.1167 ± 0.0017 for $^{207}Pb/^{206}Pb$ and $^{208}Pb/^{206}Pb$, respectively) and southern offshore core sediments (F07) (0.8435 ± 0.0004 and 2.0946 ± 0.0007 for $^{207}Pb/^{206}Pb$ and $^{208}Pb/^{206}Pb$, respectively), which were distributed south

of 36.5°N.

These mixing series might have been created by the mixing of two endmembers, consisting of an admixture of anthropogenic and natural origin or the mixing of Pb sources from different geographic regions. In the case of group 1 sediments, Pb in surface sediments was considered a mixture of current Han River sediments (combined anthropogenic and natural origin) and deep (40–65 cm) sediments (natural origin) presumed to have been deposited in the past. Based on the relationship between $^{208}Pb/^{206}Pb$ and $Cs/Pb_{leached}$, which is another indicator of a mixing relationship (Choi et al. 2007), the mixing of present and past sediments could be confirmed because $Cs/Pb_{leached}$ in the upper sediments was higher than in sediments deposited in the past in both cores YC2 and YC5 (Figs. 4 and 6b) and the $^{208}Pb/^{206}Pb$ ratios in the upper sediments of these cores were close to those in sediments from the mouth of the Han River. In this plot, sandy sediments (Cs < 2 mg/kg) were excluded because the trend between the $Pb_{leached}$ concentration and Cs could differ depending on grain size. Therefore, it is possible that all of the group 1 sediments originated from the Han River, with mixtures of past and present deposits being uncontaminated and contaminated with regard to Pb, respectively, and distributed north of 36.5°N, including Gyeonggi Bay and the offshore area. Because Pb isotopes in the group 2 sediments were confined between those of the Geum River sediments and offshore core sediments, it is possible that Pb in surface sediments south of 36.5°N was derived from the two sources. In addition, the relationship between isotope ratios and $Cs/Pb_{leached}$ for all surface and core sediments in the south indicated a mixing between Pb with anthropogenic and natural origins, as evidenced by the similar variation in the Pb isotope ratio and $Cs/Pb_{leached}$ (Fig. 6c). In this plot, four samples with high concentrations of Mn (Fig. 5b and 5c) were excluded. Therefore, natural Pb originating from the Geum River was deposited in the southernmost offshore sediments, and then anthropogenic Pb from the same river was deposited more recently, and similar geographic gradients of isotope ratio and Pb concentration were obtained. If this hypothesis is accepted, the evidence would be present in the core sediments. The $^{207}Pb/^{206}Pb$ and $^{208}Pb/^{206}Pb$ ratios were 0.8516 ± 0.0006 and 2.1164 ± 0.0011 for C1 (n = 11), 0.8509 ± 0.0007 and 2.1141 ± 0.0017 for YC11 (n = 7), 0.8458 ± 0.0016 and 2.1068 ± 0.0017 for YC13 (n = 9), 0.8445 ± 0.0004 and 2.1032 ± 0.0004 for YGC12 (n = 10), 0.8429 ± 0.0004 and 2.0997 ± 0.0009 for YGC16 (n = 8), and 0.8449 ± 0.0003 and 2.1005 ± 0.0011 for S2 (n = 8). Although the Pb isotope ratios were significantly different among cores, there was little variability within each core (length: 45–65 cm), and there was a gradual decrease in the mean isotope ratio of each core toward the south and offshore areas (Figs. 4 and 6c). Thus, no mixing relationship between Pb with anthropogenic and natural origins, such as those observed in the north, was identified in the south because anthropogenic sources from the Geum River could not be distinguished from natural sources even in cores (YC11 and C1) near the Geum River, and the range and mean values of isotope ratios and $Cs/Pb_{leached}$ in core sediments gradually decreased from the Geum River to the southern offshore area. Therefore, the mixing relationship in group 2 sediments could be interpreted as the mixing of two different sources with a high Pb isotope ratio and Pb concentration (the Geum River), and a low ratio and concentration (offshore), and not a mixing of anthropogenic and natural sources.

Tracers of fine-grained sediment sources in the southwestern Yellow Sea

The origin of fine-grained sediments has been widely investigated to study the marine environment and to trace the transport pathways of pollutants (Aoki 1976; Windom 1976; Karlin 1980; Hume and Nelson 1986). In the Yellow Sea, many studies have focused on the origin of mud deposits, such as the central Yellow Sea mud, the old Huanghe Delta mud, the northern Yellow Sea mud, and the HMB (DeMaster et al. 1985; Alexander et al. 1991b; Jin and Chough 1998; Cho et al. 1999; Park et al. 2000; Lee and Chu 2001; Yang et al. 2004; Lim et al. 2013, 2015; Um et al. 2015). Geochemical tracers such as rare earth elements (REEs), major and trace metals, and clay mineralogy have been used to identify the sources and mixing features of several sources. This study suggests a new fine-particle tracer, the Pb isotope ratio ($^{207}Pb/^{206}Pb$ and $^{208}Pb/^{206}Pb$), for use in the identification of sources for mud deposits in the southwestern Yellow Sea. Because the $Pb_{leached}$ concentration increased depending on the Pb content of fine-grained sediments and was associated with Fe oxy/hydroxide (which is fairly immobile in oxic/dynamic oceanographic conditions, such as in the Yellow Sea), and Pb isotope ratios were little affected by physicochemical fractionation processes, Pb isotopes can be used as a fine-particle tracer as well as to determine the sources and pathways of Pb (Bollhöfer and Rosman 2000, 2001; Veysseyre et al. 2001). Although Pb sources were not always consistent with the behavior of fine particles, most river-borne Pb should be

associated with fine particles once they leave the estuarine/coastal area. Therefore, $Pb_{leached}$ in coastal and offshore sediments was transported and deposited through its association with fine-grained particles. In addition, Pb isotopes could differ between different anthropogenic sources, even within the same geographic source, such as the group 1 sediments in this study. However, when Pb isotopes in the leached fraction of sediments indicate a mixing relationship among different geographic sources, such as the group 2 sediments in this study, Pb isotopes could be used as a source tracer of fine-grained sediments.

Because two sources (i.e., two endmembers) were identified and all of the samples in group 2 sediments were a mixture of materials from two sources, the relative contribution from each endmember could be estimated using the following simple binary mixing equation:

$$F_G \times (^{208}Pb/^{206}Pb)_G + F_O \times (^{208}Pb/^{206}Pb)_O = (^{208}Pb/^{206}Pb)_M$$

where F_G is the percentage of materials from the Geum River, F_O is the percentage of materials from offshore, and $(^{208}Pb/^{206}Pb)_{G,O,M}$ is the isotope ratio of each endmember (G, O) and mixture (M).

Figure 7 shows the spatial distribution of the relative contribution of materials from the Geum River. Pure materials (> 80%) were distributed northward from the river mouth, including Chunsu Bay and the offshore area. This did not mean that most sediments from the Geum River were transported northward, but it did indicate that there were no other sources. The relative contribution of the Geum River-borne materials decreased southward according to the distance from the Geum River, with the 50% contour line found at about 35.2°N (not shown). Although materials originating from the Geum River have been transported northward based on the grain size distribution (Cho et al. 1993) and the movement of a less saline water mass (Shin et al. 2002), direct evidence of the presence of the Geum River materials using a tracer of fine-grained sediments has not been previously reported. The decrease in the percentage contribution toward the south indicates that some materials from other sources were mixed with those from the Geum River. Interestingly, south of 35°N, the contribution of the Geum River-borne materials was higher offshore than in coastal areas and the 40% contour line ran in a northeast–southwest direction, not an east–west direction. The lowest (about 20%) relative contribution of the Geum River borne materials was observed around the coastal area near Mokpo, because Pb isotope ratios in this coastal area

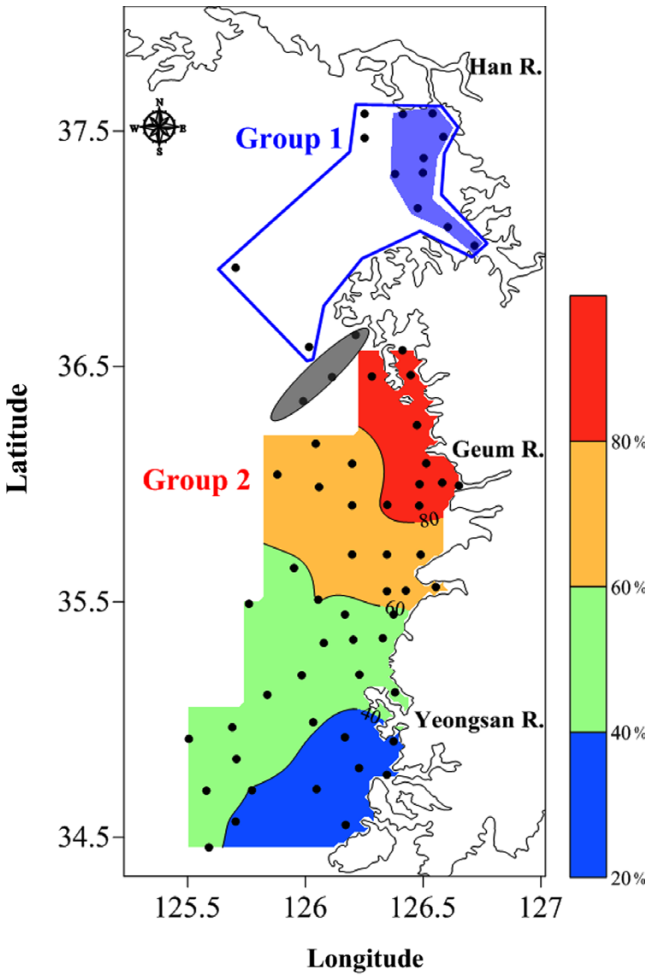

Fig. 7. Spatial distribution of the relative percentage of materials originating from the Geum River estimated using a two endmembers mixing equation for the mixing of two sources (the Geum River and offshore). The area boundary for group 1 sediments is shown, and mixtures of materials originating from the Han and Geum rivers are presented as a gray ellipse

were similar to those in an offshore core (F07). Thus, it is possible that fine-grained sediments from the Geum River were transported in the offshore direction south of 35°N and deposited at the HMB. Furthermore, there have been several reports that fine-grained sediments from offshore sources are supplied from the south to the north, and that HMB deposits consist of materials from two sources, i.e., the Geum River and Chinese rivers (Alexander et al. 1991b; Park et al. 2000; Um et al. 2015). However, the relative percentage of fine-grained sediments from the Geum River in the offshore area was about 50%, much higher than the percentages (4.2–15.7%; Um et al. 2015) estimated using an REE fractionation tracer, which might be caused by a difference in the analyzed

materials, which were bulk in this study but a <15 μm fraction in Um et al. (2015). Although it has been reported in several studies that the HMB consists of materials derived from two sources, the origin of fine-grained sediments in the coastal area near Mokpo has not been reported. This study suggests that materials from offshore areas were transported to the coastal area, although the possibility that they were derived from the Youngsan River cannot be ignored, because Pb isotope data for materials from the Youngsan River were not acquired.

6. Conclusions

The Pb concentration and Pb isotopes in the 1 M HCl leached fraction of surface and core Yellow Sea sediments collected along the Korean coast were investigated to identify the Pb source and the factors controlling the Pb concentration in sediments. The $Pb_{leached}$ concentrations had a similar geographic distribution as fine-grained sediments, while the Pb_{res} concentration had a similar spatial distribution as that of coarse-grained sediments. Based on the relationships between the $Pb_{leached}$ and Fe/Mn concentration, $Pb_{leached}$ was presumed to be associated with Mn oxide as well as Fe oxy/hydroxide. Because the Pb_{res} and K concentrations were correlated, it is possible that Pb could be hosted in a lattice of K-containing minerals such as K-feldspar.

The Pb isotope ratios in all core and surface sediments in the study area were confined within four possible endmembers in a ratio–ratio plot of three isotopes ($^{207}Pb/^{206}Pb$ and $^{208}Pb/^{206}Pb$) and were categorized into two mixing groups. One group contained the Han River mouth sediments and past deposits found at 40–65 cm in core sediments (YC2 and YC5), while the other group contained sediments confined by two endmembers (the Geum River mouth and offshore sediments). They were geographically divided into areas north (group 1) and south (group 2) of 36.5°N. For group 1 sediments, because $^{208}Pb/^{206}Pb$ and $Cs_t/Pb_{leached}$ were inversely correlated, it could be interpreted that Pb in the sediments of this group consisted of a mixture between natural and anthropogenic sources from the same origin, i.e., the Han River. This suggests that a large anthropogenic Pb input from metropolitan cities would be expected. Group 2 sediments were spatially distributed south of 36.5°N and consisted of two endmembers, i.e., the Geum River and offshore core sediments (F07). However, because all five cores had a vertically identical Pb isotope distribution and their values gradually decreased from north to south, the mixing relationship could be interpreted as sediments that were mixtures from two different geographic sources. One source had a high Pb isotope ratio and Pb concentration (the Geum River) and a low ratio and concentration (offshore), unlike group 1 sediments. Based on the two endmembers mixing model, the relative contribution of materials from the Geum River was estimated, and this indicated that Pb isotopes could be a tracer of fine-grained sediments in the Yellow Sea along the Korean coast.

Acknowledgements

This study was financially supported by Research Fund of Chungnam National University in 2014. Surface sediments (89) were provided from Library of Marine Samples of KIOST. The authors would like to thank the anonymous reviewers and editor for their insightful comments.

References

Ahn IY, Kang YC, Choi JW (1995) The influence of industrial effluents on intertidal benthic communities in Panweol, Kyeonggi Bay (Yellow Sea) on the west coast of Korea. Mar Pollut Bull **30**:200–206

Alexander CR, DeMaster DJ, Nittrouer CA (1991a) Sediment accumulation in a modern epicontinental–shelf setting: the Yellow Sea. Mar Geol **98**:51–72

Alexander CR, Nittrouer CA, Demaster DJ, Park YA, Park SC (1991b) Macrotidal mudflats of the southwestern Korean Coast: a model for interpretation of intertidal deposits. J Sediment Res **61**:805–824

Alyazichi YM, Jones BG, McLean E (2015) Source identification and assessment of sediment contamination of trace metals in Kogarah Bay, NSW, Australia. Environ Monit Assess **187**:1–10

Aoki S (1976) Clay mineral distribution in sediments of the Gulf of Thailand and the South China Sea. J Oceanogr Soc Japan **32**:169–174

Baek SH, Ki JS, Katano T, You K, Park BS, Shin HH, Shin KS, Kim YO, Han MS (2011) Dense winter bloom of the dinoflagellate Heterocapsa triquetra below the thick surface ice of brackish Lake Shihwa, Korea. Phycol Res **59**:273–285

Bargar JR, Brown GE, Parks GA (1997) Surface complexation of Pb (II) at oxide–water interfaces: II. XAFS and bond–valence determination of mononuclear Pb (II) sorption products and surface functional groups on iron oxides. Geochim Cosmochim Ac **61**:2639–2652

Bollhöfer A, Rosman KJR (2000) Isotopic source signatures for atmospheric lead: the Southern Hemisphere. Geochim Cosmochim Ac **64**:3251–3262

Bollhöfer A, Rosman KJR (2001) Isotopic source signatures for atmospheric lead: the Northern Hemisphere. Geochim Cosmochim Ac **65**:1727–1740

Calvert SE (1976) The mineralogy and geochemistry of near–shore sediments. In: Riley JP, Chester R (eds) Chemical oceanography. Academic Press, New York, pp 187–271

Carpenter RH, Pope TA, Smith RL (1975) Fe–Mn oxide coatings in stream sediment geochemical surveys. J Geochem Explor **4**:349–363

Cheng H, Hu Y (2010) Lead (Pb) isotopic fingerprinting and its applications in lead pollution studies in China: a review. Environ Pollut **158**:1134–1146

Cho YG, Lee CB, Choi MS (1999) Geochemistry of surface sediments off the southern and western coasts of Korea. Mar Geol **159**:111–129

Cho YG, Lee CB, Park YA, Kim DC, Kang HJ (1993) Geochemical characteristics of surface sediments in the eastern part of the Yellow Sea and the Korean West Coast. Korean J Quat Res **7**:69–91

Choi JK, Lee EH, Noh JH, Huh SH (1997) The study on the phytoplankton bloom and primary productivity in lake Shihwa and adajcent coastal areas. J Korean Soc Oceanogr **2**:78–86

Choi MS, Chun JH, Woo HJ, Yi HI (1999) Change of heavy metals and sediment facies in surface sediments of the Shihwa Lake. J Korean Environ Sci Soc **8**:593–600

Choi MS, Yi HI, Yang SY, Lee CB, Cha HJ (2007) Identification of Pb sources in Yellow Sea sediments using stable Pb isotope ratios. Mar Chem **107**:255–274

Chough SK, Kim DC (1981) Dispersal of fine–grained sediments in the southeastern Yellow Sea; a steady–state model. J Sediment Res **51**:721–728

Chough SK, Lee HJ, Yoon SH (2000) Marine geology of Korean seas. Elsevier, Amsterdam, 328 p

DeMaster DJ, McKee BA, Nittrouer CA, Qian J, Cheng G (1985) Rates of sediment accumulation and particle reworking based on radiochemical measurements from continental shelf deposits in the East China Sea. Cont Shelf Res **4**:143–158

Dong D, Derry LA, Lion LW (2003) Pb scavenging from a freshwater lake by Mn oxides in heterogeneous surface coating materials. Water Res **37**:1662–1666

Dong LX, Su JL, Wang KS (1989) Tide current in the Yellow Sea and its relationship with sediment transport. Acta Oceanol Sin **11**:102–114

Ewais TA, Grant A, Fattah ATA (2000) The role of surface coatings on sediments in sediment: water partitioning of trace elements and radionuclides. J Environ Radioactiv **49**:55–64

Flegal AR, Rosman KJR, Stephenson MD (1987) Isotope systematics of contaminant leads in Monterey Bay. Environ Sci Technol **21**:1075–1079

Gao S, Park YA, Zhao YY, Qin YS (1996) Transport and resuspension of fine-grained sediments over the southeastern Yellow Sea. In: Proceedings of the Korean–China international seminar on Holocene and late Pleistocene environments in the Yellow Sea Basin, Seoul National University, Seoul, Korea, 20–22 Nov, pp 83–98

Gao X, Zhou F, Chen C–TA (2014) Pollution status of the Bohai Sea: an overview of the environmental quality assessment related trace metals. Environ Int **62**:12–30

Gao Y, Arimoto R, Duce RA, Lee DS, Zhou MY (1992) Input of atmospheric trace elements and mineral matter to the Yellow Sea during the spring of a low–dust year. J Geophys Res **97**:3767–3777

Gerritse RG, Wallbrink PJ, Murray AS (1998) Accumulation of phosphorus and heavy metals in the Swan–Canning Estuary, Western Australia. Estuar Coast Shelf S **47**:165–179

Gibbs RJ (1973) Mechanisms of trace metal transport in rivers. Science **180**:71–73

Hamelin B, Grousset F, Sholkovitz ER (1990) Pb isotopes in surficial pelagic sediments from the North Atlantic. Geochim Cosmochim Ac **54**:37–47

Hamilton EI, Clifton RJ (1979) Isotopic abundances of lead in estuarine sediments, Swansea Bay, Bristol Channel. Estuar Coast Mar Sci **8**:271–278

Hao Y, Guo Z, Yang Z, Fan D, Fang M, Li X (2008) Tracking historical lead pollution in the coastal area adjacent to the Yangtze River Estuary using lead isotopic compositions. Environ Pollut **156**:1325–1331

Hinrichs J, Dellwig O, Brumsack HJ (2002) Lead in sediments and suspended particulate matter of the German Bight: natural versus anthropogenic origin. Appl Geochem **17**:621–632

Hu NJ, Huang P, Liu J, Shi X, Ma D, Zhu A, Zhang J, Zhang H, He L (2015a) Tracking lead origin in the Yellow River Estuary and nearby Bohai Sea based on its isotopic composition. Estuar Coast Shelf S **163**:99–107

Hu NJ, Huang P, Zhang H, Zhu A, He, L, Zhang J, Liu J, Shi X, Ma D (2015b) Tracing the Pb origin using stable Pb isotope ratios in sediments of Liaodong Bay, China. Cont Shelf Res **111**:268–278

Hu X, Ding Z, Liu X, Yao F, Lian H (2013) Lead content and isotope composition in surface sediments in Western Xiamen Bay and its vicinity: implication for possible source. Asian J Chem **25**:3229

Hume TM, Nelson CS (1986) Distribution and origin of clay minerals in surficial shelf sediments, western North Island, New Zealand. Mar Geol **69**:289–308

Jeong YH, Yang JS (2015) The long–term variations of water qualities in the Saemangeum salt–water lake after the Sea–dike construction. J Korean Soc Mar Environ Energy **18**:51–63

Jin JH, Chough SK (1998) Partitioning of transgressive deposits in the southeastern Yellow Sea: a sequence stratigraphic interpretation. Mar Geol **149**:79–92

Jung HS, Lee CB, Cho YG, Kang JK (1996) A mechanism for the

enrichment of Cu and depletion of Mn in anoxic marine sediments, Banweol Intertidal Flat, Korea. Mar Pollut Bull **32**:782–787

Karlin R (1980) Sediment sources and clay mineral distributions off the Oregon Coast. J Sediment Petrol **50**:543–559

Kim G, Yang HS, Kodama Y (1998) Distributions of transition elements in the surface sediments of the Yellow Sea. Cont Shelf Res **18**:1531–1542

Kim KT, Shin HS, Lim CR, Cho YG, Hong GH, Kim SH, Yang DB, Choi MS (2000) Geochemistry of Pb in surface sediments of the Yellow Sea: contents and speciation. J Korean Soc Oceanogr **35**:178–191

Klein GD, Park YA, Chang JH, Kim CS (1982) Sedimentology of a subtidal, tide–dominated sand body in the Yellow Sea, southwest Korea. Mar Geol **50**:221–240

Kober B, Wessels M, Bollhöfer A, Mangini A (1999) Pb isotopes in sediments of Lake Constance, Central Europe constrain the heavy metal pathways and the pollution history of the catchment, the lake and the regional atmosphere. Geochim Cosmochim Ac **63**:1293–1303

Koons RD, Helmke PA, Jackson ML (1980) Association of trace elements with iron oxides during rock weathering. Soil Sci Soc Am J **44**:155–159

Labonne M, Ben Othman D, Luck JM (1998) Recent and past anthropogenic impact on a mediterranean lagoon: lead isotope constraints from mussel shells. Appl Geochem **13**:885–892

Lee CB, Jung HS, Jeong KS (1992) Distribution of some metallic elements in surface sediments of the southeastern Yellow Sea. J Korean Soc Oceanogr **27**:55–65

Lee CH, Lee BY, Chang WK, Hong S, Song SJ, Park J, Kwon BO, Khim JS (2014) Environmental and ecological effects of lake Shiwha reclamation project in South Korea: a review. Ocean Coast Manage **102**:545–558

Lee HJ, Jeong KS, Han SJ, Bahk KS (1988) Heavy minerals indicative of holocene transgression in the southeastern Yellow Sea. Cont Shelf Res **8**:255–266

Lee HJ, Chough SK (1989) Sediment distribution, dispersal and budget in the Yellow Sea. Mar Geol **87**:195–205

Lee HJ, Chu YS (2001) Origin of inner–shelf mud deposit in the southeastern Yellow Sea: Huksan Mud Belt. J Sediment Res **71**:144–154

Lee HJ, Ryu SO (2008) Changes in topography and surface sediments by the Saemangeum dyke in an estuarine complex, west coast of Korea. Cont Shelf Res **28**:1177–1189

Lee HJ, Lee SH (2012) Geological consequences of the Saemangeum Dyke, mid–west coast of korea: a review. Ocean Sci J **47**:395–410

Lee HJ (2015) A review on the Holocene evolution of an inner–shelf mud deposit in the southeastern Yellow Sea: the Huksan Mud Belt. Ocean Sci J **50**:615–621

Lim DI, Choi JY, Jung HS, Choi HW, Kim YO (2007) Natural background level analysis of heavy metal concentration in Korean coastal sediments. Ocean Polar Res **29**:379–389

Lim DI, Choi JY, Shin HH, Rho KC, Jung HS (2013) Multielement geochemistry of offshore sediments in the southeastern Yellow Sea and implications for sediment origin and dispersal. Quatern Int **298**:196–206

Lim DI, Xu Z, Choi J, Li T, Kim SY (2015) Holocene changes in detrital sediment supply to the eastern part of the central Yellow Sea and their forcing mechanisms. J Asian Earth Sci **105**:18–31

Liu B, Hu K, Jiang Z, Yang J, Luo X, Liu A (2011) Distribution and enrichment of heavy metals in a sediment core from the Pearl River Estuary. Environ Earth Sci **62**:265–275

Loring DH (1990) Lithium–a new approach for the granulometric normalization of trace metal data. Mar Chem **29**:155–168

Martin JM, Zhang J, Shi MC, Zhou Q (1993) Actual flux of the Huanghe (yellow river) sediment to the Western Pacific Ocean. Neth J Sea Res **31**:243–254

Milliman JD, Beardsley RC, Zuo SY, Limeburner R (1985) Modern Huanghe–derived muds on the outer shelf of the East China Sea: identification and potential transport mechanisms. Cont Shelf Res **4**:175–188

Milliman JD, Yun SQ, Mei ER, Saito Y (1987) Man's influence on the erosion and transport of sediment by Asian rivers: the Yellow River (Huanghe) example. J Geol **95**:751–762

Munksgaard NC, Batterham GJ, Parry DL (1998) Lead isotope ratios determined by ICP–MS: investigation of anthropogenic lead in seawater and sediment from the Gulf of Carpentaria, Australia. Mar Pollut Bull **36**:527–534

Nagano T, Yanase N, Tsuduki K, Nagao S (2003) Particulate and dissolved elemental loads in the Kuji River related to discharge rate. Environ Int **28**:649–658

Négrel P, Petelet GE (2012) Isotopic evidence of lead sources in Loire River sediment. Appl Geochem **27**:2019–2030

Ng A, Patterson CC (1982) Changes of lead and barium with time in California off–shore basin sediments. Geochim Cosmochim Ac **46**:2307–2321

Park SC, Lee SD (1994) Depositional patterns of sand ridges in tide–dominated shallow water environments: Yellow Sea Coast and South Sea of Korea. Mar Geol **120**:89–103

Park SC, Lee HH, Han HS, Lee GH, Kim DC, Yoo DG (2000) Evolution of late Quaternary mud deposits and recent sediment budget in the southeastern Yellow Sea. Mar Geol **170**:271–288

Park YA, Khim BK (1992) Origin and dispersal of recent clay minerals in the Yellow Sea. Mar Geol **104**:205–213

Patterson CC (1955) The Pb207/Pb206 ages of some stone meteorites. Geochim Cosmochim Ac **7**:151–153

Ren ME, Shi YL (1986) Sediment discharge of the Yellow River (China) and its effect on the sedimentation of the Bohai and the Yellow Sea. Cont Shelf Res **6**:785–810

Schubel JR, Shen HT, Park MJ (1984) A comparison of some

characteristic sedimentation processes of estuaries entering the Yellow Sea. In: Park YA, Pilkey OH, Kim SW (eds) Proc. Korea-U. S. Seminar and workshop on marine geology and physical processes of the Yellow Sea, Seoul, pp 286–308

Shin EJ, Lee SH, Choi JY (2002) Numerical model study for structure and distribution of the Keum River plume. J Korean Soc Oceanogr **7**:157–170

Shirahata H, Elias RW, Patterson CC, Koide M (1980) Chronological variations in concentrations and isotopic compositions of anthropogenic atmospheric lead in sediments of a remote subalpine pond. Geochim Cosmochim Ac **44**:149–162

Sindern S, Tremöhlen M, Dsikowitzky L, Gronen L, Schwarzbauer J, Siregar TH, Ariyani F, Irianoto HE (2016) Heavy metals in river and coast sediments of the Jakarta Bay region (Indonesia)–geogenic versus anthropogenic sources. Mar Pollut Bull **110**:624–633

Song YH, Choi MS, Ahn YW (2011) Trace metals in Chun–su Bay sediments. J Korean Soc Oceanogr **16**:169–179

Song YH, Choi MS, Lee JY, Jang DJ (2014) Regional background concentrations of heavy metals (Cr, Co, Ni, Cu, Zn, Pb) in coastal sediments of the South Sea of Korea. Sci Total Environ **482–483**:80–91

Sutherland RA (2002) Comparison between non–residual Al, Co, Cu, Fe, Mn, Ni, Pb and Zn released by a three–step sequential extraction procedure and a dilute hydrochloric acid leach for soil and road deposited sediment. Appl Geochem **17**:353–365

Tarras Wahlberg NH, Lane SN (2003) Suspended sediment yield and metal contamination in a river catchment affected by El Nino events and gold mining activities: the Puyango river basin, southern Ecuador. Hydrol Process **17**:3101–3123

Um IK, Choi MS, Lee GS, Chang TS (2015) Origin and depositional environment of fine-grained sediments since the last glacial maximum in the southeastern Yellow Sea: evidence from rare earth elements. Geo-Mar Lett **35**:421–431

Veysseyre AM, Bollhöfer AF, Rosman KJR, Ferrari CP, Boutron CF (2001) Tracing the origin of pollution in French Alpine snow and aerosols using lead isotopic ratios. Environ Sci Technol **35**:4463–4469

Wells JT (1988) Distribution of suspended sediment in the Korea Strait and southeastern Yellow Sea: onset of winter monsoons. Mar Geol **83**:273–284

Windom HL (1976) Lithogenous material in marine sediments. Chem Oceanogr **5**:103–135

Yang CS (1989) Active, moribund and buried tidal sand ridges in the East China Sea and the Southern Yellow Sea. Mar Geol **88**:97–116

Yang SY, Jung HS, Lim D, Li CX (2003) A review on the provenance discrimination of sediments in the Yellow Sea. Earth-Sci Rev **63**:93–120

Yang SY, Lim DI, Jung HS, Oh BC (2004) Geochemical composition and provenance discrimination of coastal sediments around Cheju Island in the southeastern Yellow Sea. Mar Geol **206**:41–53

Yih WH, Myung GO, Yoo YD, Kim YG, Jeong HJ (2005) Semiweekly variation of spring phytoplankton community in relation to the freshwater discharges from Keum River estuarine weir, Korea. J Korean Soc Oceanogr **10**:154–163

Yoo YD, Jeong HJ, Shim JH, Park JY, Lee KJ, Yih WH, Kweon HK, Pae SJ, Park JK (2002) Outbreak of red tides in the coastal waters off the Southern Saemankeum areas, Jeonbuk, Korea; 1. Temporal and spatial variations in the phytoplankton community in the summer–fall of 1999. J Korean Soc Oceanogr **7**:129–139

Yu R, Zhang W, Hu G, Lin C, Yang Q (2016) Heavy metal pollution and Pb isotopic tracing in the intertidal surface sediments of Quanzhou Bay, southeast coast of China. Mar Pollut Bull **105**:416–421

Yuan H, Song J, Li X, Li N, Duan L (2012) Distribution and contamination of heavy metals in surface sediments of the South Yellow Sea. Mar Pollut Bull **64**:2151–2159

Zhang G, Liu D, Wu H, Chen L, Han Q (2012) Heavy metal contamination in the marine organisms in Yantai coast, northern Yellow Sea of China. Ecotoxicology **21**:1726–1733

Zhang J, Huang WW, Liu SM, Liu MG, Yu Q, Wang JH (1992) Transport of particulate heavy metals towards the China Sea: a preliminary study and comparison. Mar Chem **40**:161–178

Zhang W, Feng H, Chang J, Qu J, Yu L (2008) Lead (Pb) isotopes as a tracer of Pb origin in Yangtze River intertidal zone. Chem Geol **257**:260–266